

# Analysis on Complex Frequency Selective Surface (FSS) using Finite Different Time Domain Method (FDTD)

H. Nornikman<sup>1</sup>, N. C. Pee<sup>2</sup>, B. H. Ahmad<sup>1</sup>, S. N. Salleh<sup>1</sup>, M. Z. A. Abd Aziz<sup>1</sup>

<sup>1</sup>Center for Telecommunication Research and Innovation (CeTRI), Faculty of Electronics and Computer Engineering (FKEKK), Universiti Teknikal Malaysia Melaka (UTeM), Durian Tunggal, Melaka, Malaysia

<sup>2</sup>Faculty of Information and Communication Technology (FTMK), Universiti Teknikal Malaysia Melaka (UTeM), Durian Tunggal, Melaka, Malaysia  
nornikman@utem.edu.my

**Abstract**—In this paper, three different situations of the symmetry frequency selective surface (FSS) shaped are designed – consist of without symmetry, 1/4 symmetry and 1/8 symmetry condition using FORTRAN software. In this work, the Energy-Saving Glass (ESG) that covered the glass with a metallic oxide coating to exploit obstructive of infrared and ultraviolet radiation into structures. The tools used in this work were applied to propose a complex shape by using Genetic Algorithm (GA) as the optimization tool to create bits of the chromosome in designing the shape of energy-saving glass (ESG). It also used the Finite Difference Time Domain (FDTD) was working as a process of numerical algorithm modeling to design the complex shape in pixelized shape based on the unit cell idea. For without symmetry complex, 1/4 symmetry complex and 1/8 complex for FSS shape, it shows that the - 43 dB at 1.2 GHz, respectively.

**Index Terms**— Finite Difference Time Domain; frequency selective surface; Genetic Algorithm; energy-saving glass; FORTRAN

## I. INTRODUCTION

Nowadays, the Frequency Selective Surface (FSS) is working in several terrestrial and electromagnetic shielding applications [1]. This structure is a repetitive patch structure element that organized in one- (1D) or two-dimensional (2D) planes [2]. By applying the FSS in the basic Energy-Saving Glass (ESG) shape, a good performance is gained in the wanted frequency. It also not changes the thermal assets close to a suitable level effect on arranged unit cell maintains static positions in the action of geometrical shapes. It is also known that this basic shape structure of FSS forward to transmission loss better 25 dB [3] for cross dipole shape.

There are many types of shape can be used in the simulation, not only focus on the basic shape of circular or square. In this case, FSS with the repeated random one-unit cell can be designed to perform larger periodic FSS patch shape. The researcher can explore the larger FSS design to achieve good absorption characteristic performance in the system.

The work of FSS has been started in the 1960s. Before that, Marconi in 1919 patented the periodic structure that focuses on FSS structure in parabolic dish antenna design. So, this structure is the best candidate to apply in the system to enhance the transmission signal to pass through energy

saving glass. The periodic structure element of the FSS provides the matching cell of single and double occupancy periodic in several directions.

There is previous research that applies FSS in their design. Suhaimi in 2018 introduced his work on health monitoring system using new 3D FSS technique that impact to increase the sensitivity compared with the 2D FSS [5]. Rahim had been designed the multi-metallic layered miniaturized-element frequency selective surfaces (MEFSSs) as a band pass characteristic at X-band up to 30 GHz. This technique effect to reduce the unit size cell compared with the conventional design [6].

Azemi had presented work on novel 3D FSS with cylinder ring unit element that resonates between 2.56 GHz and 2.67 GHz of band stop region [7]. In other work of Akbari, the planar crossed-dipole metal strips FSS had been applying in four-port circularly polarized antenna for multiple-output (MIMO) system at 30 GHz [8]. The other works on the FSS are stated in this several papers [9-10].

The FSS can be shown as a periodic array of elements on a planar surface that resonating at a single or multiple frequency ranges. In this case, the length of elements is a multiple of half of the resonant wavelength as Equation (1) [11]:

$$\lambda_g/2 \quad (1)$$

It also shows that the patches with comparable shapes are can called as periodic. Consequently, the calculated electromagnetic waves absorbed performance of FSS patches are approve using the concept of Periodic Boundary Condition (PBC). Besides that, Yee's Cell concept can be used in FDTD technique. This work can be done by dividing one-unit cell of FSS to effect the calculation of FDTD that control the electromagnetic waves absorbed through the FSS patches [12].

Additionally, there are many to produce ways multi-band effect in FSS, such as using multi elements unit cells and design using basic method of Genetic Algorithm (GA). Next, this periodic structure of the complex unit cell capability to perform for manipulating the FSS design with multiband effect. To acquire the best transmission, the random design of analogous design geometries and numerous size or with fragmented geometries had widely used [13].

Basically, the FSS are creating at the front side of the dielectric slab to generate substrates [14]. These substrates exhibited the high impedance in absorbing surface platform. Furthermore, the formation of FSS patch can be designed in various shape that effect to perform different volumes of microwave absorption rate [15].

In the meantime, in the work of software simulation, there is no limitation to produce a new structure of FSS beside the basic conventional structure. The simulation software has a capability to produce a random computerized shaped of one-unit cell shaped that difficult to design by normal conventional technique. This repeated random shaped can form a big and complex FSS system to perform an investigation to measure the FSS absorption characteristic performance [16].

In addition, the replication of random unit cell of complex FSS design is constructed on the dimension size of ESG. For the sample, ESG necessitates an array replication system, such as quarter (1/4) shape or half (1/2) shape, to accomplish all the glasses as symmetrical FSS periodic unit [17]. After that, the implementation of the Floquet PBC with FDTD method must be done to make sure the acceptable analysis of FSS. Before that, the significant symmetrical condition is the important part before proceeding with the FSS complex design. This is because the limited time convergence of GA can effect the system performance. The user typically required a decent sized population and lots of generations to perform an acceptable value with longer time simulation solution work [18].

Based on this work, there are three conditions stated used: half symmetry, quarter symmetry, and octal symmetry. Half symmetry is using a mirror concept of full shape. The full shape can be designed from the combination of half symmetry. For the quarter is the mirror concept of the half symmetry condition. The octal symmetry condition is obtaining after 1/8 image of the mirrored process done and generate the quarter shape. To generate a full shaped, two conditions before had been applying.

Currently, the Finite Different Time Domain (FDTD) is a widespread computational electromagnetic (CEM) modeling method that used by numerous researcher. One of the reason is this modelling method is user-friendly with time domain technique and cover a wide range of frequency in a single simulation work [19].

This technique is also acceptable and has a good reputation for using in simulated the metamaterial area that powerful to apply the complex periodic structures Maxwell's equation [20].

The foundation of FDTD was laid down by Yee in 1966 [21]. The spatial sampling of vector components of the electric and magnetic fields had been chosen by Yee. This work allows on behalf of mutually the differential and integral forms of Maxwell's equation in a healthy method [22].

The FDTD had the capability to solve the issues regarding time domain, but the frequency domain response still can be gained in a wide range by through the Fast Fourier Transform (FFT) technique application. This technique delivers an easy formulation that did not need complicated formulation or Green's function [20].

Consequently, FDTD is the right candidate to resolve the differential time domain in Maxwell's equation that used in this work. It is also correlated to numerical analysis that applies the numerical calculation technique in explaining the

problems.

Sudiarta had been used FDTD technique to establish energies and wave function of two-electron quantum dot using time-dependent Schrödinger equation (TDSE) [23]. In FSS area, Chen applies the alternating direction implicit FDTD to simulate his design at Terahertz frequency that had potential to control the tunable FSS [24]. Shunxi before that had done the millimeter wave FSS using FDTD technique [25].

This paper represents the result of complex shape in three types of symmetrical which are in without symmetry, 1/4 symmetry, and 1/8 symmetry. All the shape for three symmetrical is the same design and result; the difference is the value of bits chromosome and time simulation. The purpose of this design is to indicate the time simulation reduced as the value of bits chromosome decreased.

## II. ALGORITHM METHOD

For algorithm method section, it shows that the space parameters difficulties describe adjustable the problem space and the FDTD parameters.

Basically, the state the code requirements sequence represents the first stage in this work. The process of problem definition is involved of the creation of data structures that stored required information on the electromagnetic problem to be answered.

The data are containing many components such as the material used, electromagnetic properties of the material, geometries of the objects in the problem space, source types, waveform used and other specific simulation parameters of the time and dimension size of the cell [26].

The Nyquist sampling formula can be applied in this case to regulate the following a cell size of three dimensions (3D) for FSS structure. The cell size had been obtained in every direction of y and z axis, and communal parallel values with direction x, shown in Equation (1), where  $\lambda$  is lambda in meter, the speed of light in free space,  $c = 3 \times 10^8$  and  $f_H$  is the highest frequency.

The application effect the frequency used to the simulation tool. Microwave and RF signal had a frequency range between 30 kHz to 300 GHz. In this work, the application had been absolute to set the highest frequency is 6 GHz. The value of lambda had been set at 0.0015 m. This signal will transmit over the ESG that covers a frequency modulated (FM) radio until microwave oven. With these two parameters, this cell size can be estimated by separating the lambda value with the sampling value, shown in Equation (2). In FDTD technique, the sampling value is usually in the range of 10 sampling until 20 to 30 sampling [27].

$$\Delta x = \frac{\lambda}{\text{sampling}} \quad (2)$$

$$\Delta x = \frac{0.015}{30} = 0.05mm$$

This formula is determined for three axes x, y, and z where  $\Delta x = \Delta y = \Delta z$  have a common value. At that time, it shows that the amount of Yee cell to be formed to convert one-unit cell by consuming the formula in Equation (3) with

21 mm × 21 mm unit cell, based on the literature review work in [28].

$$\frac{\text{unitcell}}{\Delta x} = \frac{21\text{mm}}{0.5\text{mm}} = 42\text{yee cell} \quad (3)$$

After the cell size was once known using formula, the highest time step  $\Delta t$  directly based on the Courant condition as this simulator tool followed that the plane wave proliferated through the grid of FDTD. Utilizing this progression, any point on this wave can't go concluded many cells claiming amid the one-time step; the FDTD might proliferate the path just from one cell to its closest location unit. The Courant-Friedrichs-Lewy (CFL) condition is basically coming from the FDTD process of numerical stability. The CFL condition needs time increase with a bound with respect to the grid space increase  $\Delta t$  for the time step. Equation (4) shows the numerical strength:

$$\Delta t = \frac{1}{c \sqrt{\frac{1}{(\Delta x)^2} + \frac{1}{(\Delta y)^2} + \frac{1}{(\Delta z)^2}}} < 1 \quad (4)$$

$$\Delta t = \frac{1}{3 \times 10^8 \sqrt{\frac{1}{(0.5 \times 10^{-3})^2} + \frac{1}{(0.5 \times 10^{-3})^2} + \frac{1}{(0.5 \times 10^{-3})^2}}} < 1$$

$$\Delta t = 0.96^{-12} \text{ s}$$

Where  $c$  is the speed of light in free space,  $\Delta t$  is the time step, with  $\Delta x$ ,  $\Delta y$ , and  $\Delta z$  are the grid size of the FDTD structure.

Meanwhile, the velocity of propagation in material platform had been minor than the speed of light in free space; the CFL condition was purposeful to inhomogeneous media. Though, some issues affected the numerical stability, such as Absorbing Boundary Condition (ABC), non-parallel spatial grids, and non-linear materials [22]. Temporarily, the FDTD method had been founded on testing, and in addition refreshing the electric and attractive fields in time and space, as wave spread in the discrete matrix space may change from the ceaseless space.

Subsequently, the speed of engendering in material platform had been littler than the speed of light in free space; the CFL condition was connected to inhomogeneous media. Be that as it may, a few components influenced the numerical strength, for example, Absorbing Boundary Condition (ABC), non-uniform spatial lattices, and non-straight materials [22]. In the interim, the FDTD strategy had been founded on testing, and refreshing the electric and attractive fields in time and space, as wave proliferation in the discrete network space may contrast from the ceaseless space.

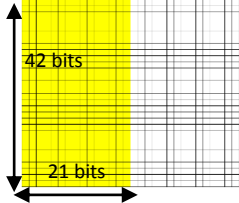
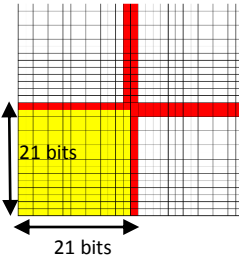
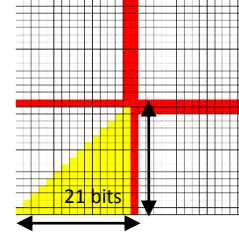
Instead, for the numerically stable FDTD technique, the time step  $\Delta t$  in ratio  $c\Delta t / \Delta u$  must be fenced to a special limit, frequently called Courant factor, where the limit hinge on both the dimension and the angle of incidence.

Table 1 demonstrates the computation for sorts of symmetrical utilized by the test system apparatus. The table beneath demonstrates the count of the quantity of bits chromosome for each sort of symmetrical. The quantity of

bits chromosome for one-unit cell or no symmetrical depends on the computation in Equation (5):

$$42 \text{ yee cell} \times 42 \text{ yee cell} = 1764 \text{ bits} \quad (5)$$

Table 1  
Computation for sorts of symmetrical utilized by the test system apparatus

symmetrical	Block outline	bits
1/2 symmetrical		42bits x 21 bits = 882 bits
1/4 symmetrical		21bits x 21 bits = 441bits
1/8 symmetrical		1bit + 2 bits + 3 bits + 4 bits + 5 bits + 6 bits + 7 bits + 8 bits + 9 bits + 10 bits + 11 bits + 12 bits + 13 bits + 14 bits + 15 bits + 16 bits + 17 bits + 18 bits + 19 bits + 20 bits + 21 bits = 231bits

By considering the aggregate bits chromosome, countless was shown, and in this way, it would set aside quite a while for iteration and simulation for the one-unit cell. Henceforth, keeping in mind the end goal to decrease time emphasis, reproduction, and the quantity of bits chromosome, frequency selective surface (FSS) was presented in this test system by utilizing the idea of symmetrical technique.

The list of symmetrical can be selected in the simulator tool such as 1/2 symmetrical (2-half), 1/4 symmetrical (4-quart), 1/8 symmetrical (8-octal), and zero (0-without symmetry), which. The faster iteration time and simulation time of the object is effect by the minimum symmetrical design process. The table beneath demonstrates the estimation of the quantity of bits chromosome for each kind of symmetrical. The minimum symmetrical would prompt speedier iteration time and recreation time of question.

### III. FSS DESIGN

GA working on the coding of the parameters, in its place of the parameters themselves. The determination the bit chromosome by GA tools focusing on the data that given by user by calculation of Yee Cell. After done, it shows the results of 21 Yee cells were used in this work.

GA, which worked as the advancement optimization device, had been created from the Matlab programming

program [29]. Kent in his paper had been applied GA in his FSS design and effect to use a short time of simulation work [30]. This enhancement was utilized for the determination activity to choose the specific genomes that experienced either hybrid or change procedure. This determination presented the impact of wellness capacity to GA advancement process, where the wellness agreed to an individual must be used in the choice activity since it alluded as the info measure of the individual chromosome.

It turned into hired to generate a population of results, and some genetic operators had been useful, which includes mutation and crossover, to conform the solutions so one can locate the first-rate one. the optimization device input delimited the quantity of Yee cells, the type of symmetry, the variety of chromosome, the type of complicated, the kind of metal chromosome, and the form of mobile used in shape on these studies, as proven in the Matlab coding in Figure 1.

```

Cell=42% input of unit cell length
sym=8 % symmetrical: 4-quart, 8-octal, 0-without symmetry
numchro=1 % the information of chromosome
random=1 % 1 - random, 0= not random
allone=0 % for unique chromosome, 1- for all chromosome is metal, 0- no chromosome is metal
HalfCell=Cell/2;
    
```

Figure 1: GA optimization code in Matlab

At that point, the kind of symmetry is ascertained in view of the info picked by the client for the quantity of bits chromosome that was produced to outline the complex (irregular) shape. Using Matlab, this simulator can create and demonstrates that the client picked 1/8 symmetry for the code. Hence, the computation of this symmetry in the simulator is portrayed in Figure 2.

```

ifsym==4
Nbits=HalfCell*HalfCell; %if quarter part symmetrical chromosome
elseifsym==8
Nbits=(HalfCell*HalfCell-HalfCell)/2+HalfCell; %if 8 part symmetrical chromosome
elseifsym==0
Nbits=Cell*Cell; %if not symmetrical chromosome
end
    
```

Figure 2: Formula that used in Matlab to compute bit

Table 2  
Number of bits and total chromosomes of FSS shape

FSS Shape	Total chromosomes	Number Bits
Without symmetry	1	1764
1/4	1	441
1/8	1	231

The FSS design with random shape is exposed in Figure 3 successfully created based on the bit chromosome *a*. In addition, many bits of the chromosome were applying; it set aside a more drawn out opportunity to reproduce this design in 162.056 seconds in one loop of iteration.

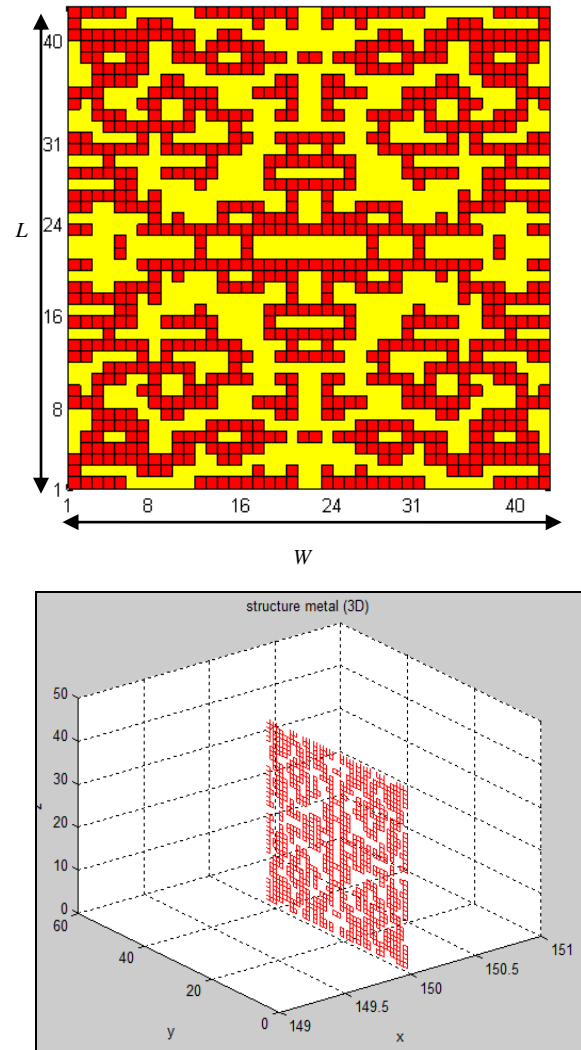


Figure 3: No symmetrical shape for FSS, (a) in two dimensional, (b) in three dimensional

#### IV. RESULT

It shows that the dimension of the length, *L*, and the width, *W*, of the FSS are 21 mm x 21 mm with a value of 42 Yee cells, with a unit cell of 0.5 mm length x 0.5 mm width in axes *y* and *z*. the complete simulation FSS shape appears in Figure 4.

The graph demonstrates that the shape had a return loss nearly 1.2 GHz for all TE oblique angles. This outcome created a bandstop at 1.2 GHz because of the signal blocking at frequencies. Consequently, the various frequencies ran between 0 GHz to 6 GHz, excluding for both bandstop frequencies that were in bandpass condition.

It shows that the return loss was lifted to -43 dB at 1.2 GHz respectively as the TE decreased. At 2.7 GHz and 4.3 GHz shows the result of -12 dB and -18 dB, respectively. The different is shows only at the first range of bandwidth; the other part remains the same results.

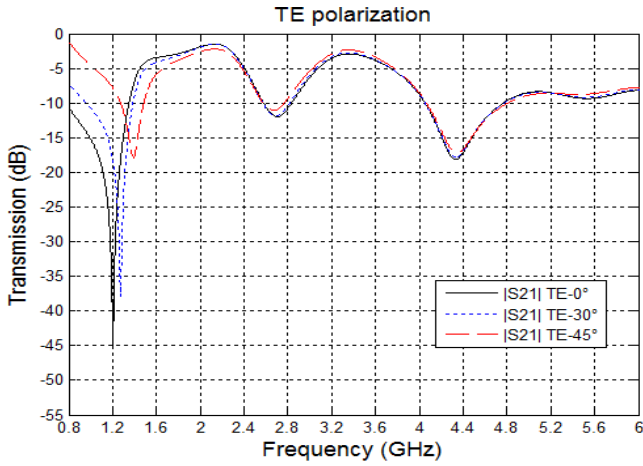


Figure 4: FSS shape with transmission coefficient for without symmetry complex

The simulation presented that 0 dB, 0 dB, and 3 dB attenuations were attained at 0°, 30°, and 45° incidence angles that reached in the range of 0 GHz and 6 GHz, while attenuations for 2.45 GHz WLAN and 5.25 GHz WLAN band at 0°, 30°, and 45° incidence generated - 5 dB and - 8 dB transmission loss as the signals were attenuated, later as long as essential wireless security. The data transmissions for this non-symmetrical shape were 1.4 GHz and 2.3 GHz at the lower and advanced frequencies individually, alluding to the - 3 dB cut off recurrence frequency.

The diagram of transmission coefficient for 1/4 symmetry complex for FSS shape is demonstrated in Figure 5. The outcomes demonstrate that the outline of the ESG shape, for the most part, showed the outcome for 1/4 symmetrical like that of without symmetrical outcome. Furthermore, there was comparable esteems for bandstop recurrence, where the started at 1.2 GHz and the end at 4.3 GHz. Instead of this plan, there were same occurrence edges at 0°, 30°, and 45° for simulated attenuation signals burrowed to the ESG.

These outcomes were gained via unit cell simulation with PBC. On the frequencies of WLAN at 2.45 GHz, the attenuations at 0°, 30°, and 45° incidences angles were 1 dB, 1 dB, and 2 dB. Then, for WLAN at 5.25 GHz at 0°, 30°, and 45° incidences angles, the transmission loss was 8 dB.

Without symmetry complex, FSS shape effect to change the transmission several at the resonance frequency. The season of reproduction contrasted for the two shapes because of demonstrated the technique for reenactment was like without symmetry shape. It shows that on account of; 1/4 symmetry shape just reproduced 1/4 from this shape contrasted with the above shape, which reenacted all shapes. For FSS complex form on a metallic oxide overlaying, these effects have been extremely promising as they showed the likelihood of preserving up WLAN imprisonment on the transmission within the coveted band.

For 1/8 shapes, the quantity of bits chromosome was not as much as both symmetrical esteems above, which influenced the time of simulation. The reason for reduction time to 81.50899786 per the second effect by only simulated 1/8 part of the FSS complex shape in unit cells.

On this element, the outcomes display the incident electromagnetic wave that immediately hit the substrate at the center part. It changes the simulation into executed type, with the response of this shape is proven in discern 6 for 3 occurrence indirect angles, which had been zero°, 30°, and 45° in TE mode polarization.

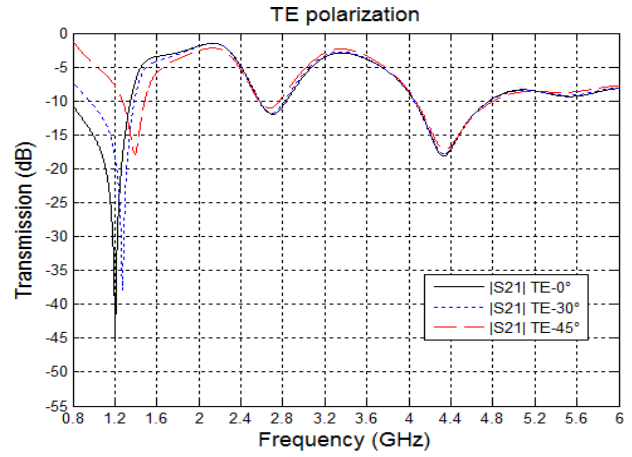


Figure 5: FSS shape with transmission coefficient for 1/4 symmetry complex

The performance of transmission diagram displayed that the lowest bandstop turned into gained at the resonant frequency of 1.2 GHz for all prevalence angles; either normal prevalence or oblique incidence, even as the very best bandstop became 4.3 GHz. the graph also illustrates that the lower frequency lifted as the indicators handed through to WLAN frequency range with a value of - 40 dB that expanded to at least 1.0 dB and 2.0 dB for 2.45 GHz WLAN at 0°, 30°, and 45° occurrence angles. the analyzing graph for 5.25 GHz with fee significance has been 8.0 dB for 0°, 30°, and 45° occurrence angles.

At this point, the outcomes demonstrate the incident electromagnetic wave that specifically knockout the substrate at the center part. Figure 6 shows the result for three diagonal rate points, which were 0°, 30°, and 45° in TE mode polarization.

The diagram of transmission diagram demonstrated that the most minimal bandstop was acquired at the resounding recurrence of 1.2 GHz for all rate points; either ordinary frequency or angled rate, while the most noteworthy bandstop was 4.3 GHz. The chart additionally demonstrates that the lower recurrence moved as the signs went over to WLAN groups with an estimation of - 40 dB that expanded to 1 dB and 2 dB for 2.45 GHz WLAN at 0°, 30°, and 45° rate points. The results for 5.25 GHz with esteem greatness had been 8 dB for 0°, 30°, and 45° frequency points.

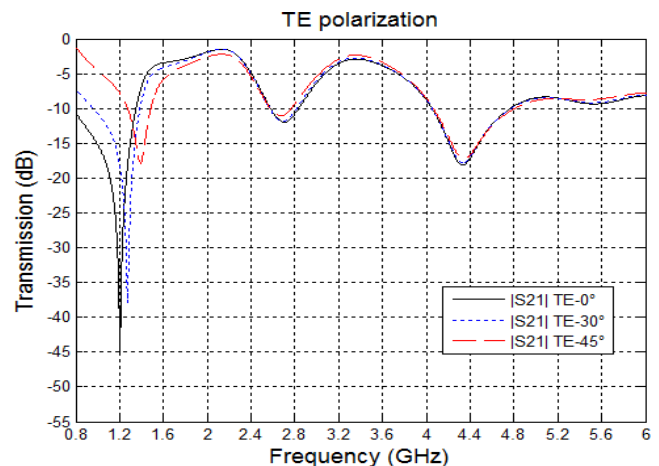


Figure 6: FSS shape with transmission coefficient for 1/8 symmetry complex

The time of simulation for without symmetry shaped, 1/4 symmetry shape and 1/8 shape are 162.056 seconds, 98.056

per second, 81.50899786 per second, respectively. In this case, it had been reduced the time for the 1/8 shaped compare without symmetry shape.

## V. CONCLUSION

In this work, three different FSS shaped are compared, starting with without symmetry shape, 1/4 symmetry shape, and 1/8 symmetry shape. From the outcomes appeared, when the state of the FSS metal reformed, the outcomes additionally changed. The outcomes were influenced by the FSS shape. Separately shape had its own characteristic which chose and hindered the signs at certain recurrence, other than enabling the signs at different frequencies to pass.

Beside FSS structure that effects the  $S_{21}$  performance, there are other significant parameters that effect this matter. In this case, dielectric constant and the thickness of the dielectric is another parameter that effect change in filtering the signals role. On the other hand, both the parameters were changed and the FDTD simulation. Furthermore, the timing also had been reduced compared with the without symmetry with 1/4 symmetry shape and 1/8 shape. By completed this work, the future researcher can be applying the new random shape to improve their FSS performance.

## ACKNOWLEDGMENT

The authors would like to thank Universiti Teknikal Malaysia Melaka (UTeM) for supporting in obtained the information and material in the development of our work. We also want to thank the Government of Malaysia which sponsoring this work under the TRGS/1/2014/FKEKK/02/1/D00001 from Ministry of Higher Education (MOHE). Thanks also to UTeM Research and Innovation Management (CRIM) for the support in publication issues. Lastly, we also thank the anonymous referees whose comments led to an improved presentation of our work.

## REFERENCES

- [1] G. I. Kiani, O. L. Karlsson, and K. Esselle, "Transmission analysis of energy saving glass windows for the purpose of providing FSS solutions at microwave frequencies," *IEEE Antennas and Propagation Society International Symposium (AP-S 2008)*, pp. 1-4, 2008
- [2] G. I. Kiani, K. L. Ford, L. G. Olsson, K. P. Esselle and C. J. Panagamuwa, "Switchable Frequency Selective Surface for Reconfigurable Electromagnetic Architecture of Buildings," in *IEEE Transactions on Antennas and Propagation*, vol. 58, no. 2, pp. 581-584, 2010.
- [3] M. Gustafsson, A. Karlsson, A. P. Rebelo, and B. Widenberg, "Design of frequency selective windows for improved indoor-outdoor communication," *IEEE Trans. Antennas Propagation*, 54, 1897-1900, 2006.
- [4] I. Ullah, "Transmission improvement of mobile phone signals through energy saving glass using frequency selective surface," 12th Australian symposium on Antenna, 2011
- [5] S. A. Suhaimi, S. N. Azemi, P. J. Soh, "Feasibility Study of Frequency Selective Surfaces for Structural Health Monitoring System," *Progress In Electromagnetics Research C*, Vol. 80, 199-209, 2018
- [6] A. F. Chan, "The Finite Difference Time Domain Method for Computational Electromagnetics," Bachelor of Engineering (Electrical and Electronic) dissertation of University of Southern Queensland, pp. 32 - 33, 2006
- [7] S. N. Azemi, K. Ghorbani, and W. S. T. Rowe, "3D Frequency Selective Surfaces," *School of Electrical and Computer Engineering, RMIT University*, vol. 29 pp. 191-203, 2012
- [8] M. Akbari, H. Abo Ghalyon, M. Farahani, A. R. Sebak and T. A. Denidni, "Spatially Decoupling of CP Antennas Based on FSS for 30-GHz MIMO Systems," in *IEEE Access*, vol. 5, pp. 6527-6537, 2017.
- [9] Y. S. Lee, F. Malek and F. H. Wee, "Investigate FSS structure effect on WIFI signal," 5th IET International Conference on Wireless, Mobile and Multimedia Networks (ICWMMN 2013), pp. 331-334, 2013
- [10] M. Bilal, R. Saleem, H. H. Abbasi, M. F. Shafique and A. K. Brown, "An FSS-Based Nonplanar Quad-Element UWB-MIMO Antenna System," in *IEEE Antennas and Wireless Propagation Letters*, vol. 16, pp. 987-990, 2017.
- [11] T. Wu, "Symmetry analysis of the nonlinear MHD equations" by *Physics Letters A*, vol: 198, pp. 467-468, 1995
- [12] S. Govindaswamy, J. East, F. Terry, E. Topsakal, J. L. Volakis, and G. I. Haddad, "Frequency-Selective Surface Based Bandpass Filters In The Near-Infrared Region," pp. 266-269, 2013
- [13] R. A. Hill and B. A. Munk, "The Effect of Perturbating a Frequency Selective Surface and Its Relation to the Design of a Dual-Band Surface," *IEEE Transactions on Antennas and Propagation*, vol. 44, no. 3, pp. 368-374, 1996.
- [14] B. A. Munk, *General Overview*, in *Frequency Selective Surfaces: Theory and Design*, John Wiley & Sons, Inc, 2000
- [15] M. Battaglia, G. Abrams, P. Denes, L.C. Greiner, B. Hooberman, L. Tompkins, H. H. Wieman, *Monolithic CMOS Pixel R&D for the ILC at LBNL*, 2005 International Linear Collider Workshop, 811, 2005
- [16] Y. Hirai, K. Yokota, and T. Momose, *Studies on the Novel Cyclodepsipeptides, "A Total Synthesis of (+)-Jaspakinolide (Jaspamide)," Heterocycles*, vol. 39, pp. 603-612, 1994
- [17] F. M. Johar, F. A. Azmin, A. S. Shibghatullah, M. K. Suaidi, B. H. Ahmad, M. Z. A. Abd Aziz, S. N. Salleh, M. Md. Shukor, "Application of Genetic Algorithm to the Design Optimization of Complex Energy Saving Glass Coating Structure," *Journal of Physics: Conference Series* 495, 2014
- [18] N. J. Radcliffe, P. D. Surry, "Fundamental Limitations on Search Algorithm: Evolutionary Computing in Perspective. *Computer Science Today: Recent Trends and Developments*", Ed: j. Van Leeuwen, Springer-Verlag LNCS 1000, pp 275-291, 1995.
- [19] J. Jinzu, K.K. Tong, H. Xue, P. Huang, "Quadratic recursive convolution (QRC) in dispersive media simulation of finite-difference time-domain (FDTD)," *Optik - International Journal for Light and Electron Optics*, vol. 138, pp. 542-549, 2017
- [20] A. Taflove, "Computational Electrodynamics: The Finite-Difference Time-Domain Method Third Edition," Norwood, MA: ArtechHouse, pp. 553-605, 2005
- [21] K. S. Yee, "Numerical solution of initial boundary value problems involving Maxwell's equations in isotropic media," *IEEE Transaction Antennas Propagation*, vol. 14, no. 3, 302-307, 1996.
- [22] Y. Wenhua, Y. Xiaoling, M. Raj, M. Akira, "Advanced FDTD Methods Parallelization," *Acceleration and Engineering Applications*. Artech House, 2011.
- [23] I. W. Sudiarta, L. M. Angraini, "The Finite Difference Time Domain (FDTD) Method to Determine Energies and Wave Functions of Two-Electron Quantum Dot," *Physics - Computational Physics*, arXiv preprint arXiv:1706.02720, 2017
- [24] J. Chen, G. Hao and Q. H. Liu, "Using the ADI-FDTD Method to Simulate Graphene-Based FSS at Terahertz Frequency," *IEEE Transactions on Electromagnetic Compatibility*, vol. 59, no. 4, pp. 1218-1223, 2017.
- [25] J. Shunxi and D. Wenbin, "FDTD Analysis of Millimeter Wave FSS," 2006 Joint 31st International Conference on Infrared Millimeter Waves and 14th International Conference on Terahertz Electronics, pp. 306-306, 2006
- [26] T. Rahim, F. A. Khan and X. Jiadong, "Design of X-band frequency selective surface (FSS) with band pass characteristics based on miniaturized unit cell," 2016 13th International Bhurban Conference on Applied Sciences and Technology (IBCAST), pp. 592-594, 2016
- [27] A. Elsherbeni, V. Demir, "The Finite-Difference Time-Domain Method for Electromagnetics with MATLAB Simulations," Scitech Publishing, INC, 2009.
- [28] K. El Mahgoub, F. Yang, A. Z. Elsherbeni, "Scattering Analysis of Periodic Structures Using Finite-Difference Time-Domain," *Morgan & Claypool*, pp. 66-70, 2012
- [29] F. M. Johar, F. A. Azmin, M. K. Suaidi, A. S. Shibghatullah, B. H. Ahmad, S. N. Salleh, M. Z. A. Abd Aziz, M. Md Shukor, "A review of Genetic Algorithms and Parallel Genetic Algorithms on Graphics Processing Unit (GPU)," 2013 IEEE International Conference on Control System, Computing and Engineering, Mindeh, 2013, pp. 264-269.

- [30] E. F. Kent, B. Doken, M. Kartal, "A New Equivalent Circuit Based FSS Design Method by Using Genetic Algorithm," 2nd International Conference on Engineering Optimization, pp. 1-4, 2010